Journal of Sports Sciences
Publication details, including instructions for authors and subscription information:
http://www.informaworld.com/smpp/title~content=t713721847

The influence of squat depth on maximal vertical jump performance

Zachary J. Domire [a]; John H. Challis [b]
[a] University of Wyoming. Laramie, WY
[b] Biomechanics Laboratory, Pennsylvania State University. University Park, PA. USA

To link to this article: DOI: 10.1080/02640410600630647
URL: http://dx.doi.org/10.1080/02640410600630647

Journal of Sports Sciences, January 15th 2007; 25(2): 193–200

The influence of squat depth on maximal vertical jump performance

ZACHARY J. DOMIRE[1] & JOHN H. CHALLIS[2]

[1]*University of Wyoming, Laramie, WY and* [2]*Biomechanics Laboratory, Pennsylvania State University, University Park, PA, USA*

(Accepted 9 February 2006)

Abstract

An increase in the period over which a muscle generates force can lead to the generation of greater force and, therefore, for example in jumping, to greater jump height. The aim of this study was to examine the effect of squat depth on maximum vertical jump performance. We hypothesized that jump height would increase with increasing depth of squat due to the greater time available for the generation of muscular force. Ten participants performed jumps from preferred and deep squat positions. A computer model simulated jumps from the different starting postures. The participants showed no difference in jump height in jumps from deep and preferred positions. Simulated jumps produced similar kinematics to the participants' jumps. The optimal squat depth for the simulated jumps was the lowest position the model was able to jump from. Because jumping from a deep squat is rarely practised, it is unlikely that these jumps were optimally coordinated by the participants. Differences in experimental vertical ground reaction force patterns also suggest that jumps from a deep squat are not optimally coordinated. These results suggest there is the potential for athletes to increase jump performance by exploiting a greater range of motion.

Keywords: *Computer simulation, biomechanics, coordination, jumping*

Introduction

Maximum vertical jumping has received considerable attention in the biomechanics literature (e.g. Alexander, 1990; Challis, 1998; Van Soest, Schwab, Bobbert, & Van Ingen Schenau, 1993), and much is known about optimal performance (Pandy & Zajac 1991). The increase in jump height for jumps commenced with a countermovement, compared with jumps begun from an initial squat position, has been attributed to the longer duration of the countermovement jump, which allows greater muscular force to be generated (Bobbert, Gerritsen, Litjens, & Van Soest, 1996). In squat start jumps, increasing the depth of squat should have a similar effect as a countermovement on the muscles involved, and therefore should result in greater jump heights. No study to date has explicitly examined the influence of initial squat depth on jump height.

Selbie and Caldwell (1996) used a simulation model to assess the effect of initial position on countermovement jump height. Initial position had only a small effect on jump height, but these were countermovement jumps and the bottom-most position in the jumps was very similar for all jumps irrespective of initial position. Van Soest, Bobbert and Van Ingen Schenau (1994) used a direct dynamics simulation to investigate how muscle model activation patterns influence jumps made from different initial positions. Muscle activation was optimized to determine maximum jump height from each initial posture examined. A global optimal activation pattern for jumps from different initial positions was also established. This activation pattern was one that would maximize the sum of the jump heights from each position. Jumps using the global optimization pattern were close to the optimal jump height for each position tested. Van Soest *et al.* (1994) suggested that jumping from a deeper initial squat might not require significant changes in muscle activation patterns. However, when jumps were optimally activated from deep squats, jump height was higher than in the preferred position.

Several studies have indicated that jump height may not be influenced by initial squat positions, but none of these studies systematically examined the influence of squat depth on jump height. The aim of this study was to examine the effect of squat depth on maximum vertical jump performance, using both an experimental and a modelling approach. We

Correspondence: Z. J. Domire, 110 Corbett Building, University of Wyoming, Laramie, WY 82071, USA. E-mail: zdomire@uwyo.edu

ISSN 0264-0414 print/ISSN 1466-447X online © 2007 Taylor & Francis
DOI: 10.1080/02640410600630647

hypothesized that jump height would increase with increasing depth of squat, due to the greater time available for the generation of muscular force.

Methods

In the following sub-sections, details are provided of the experimental and modelling approaches used to analyse the jumps.

Experimental analysis

Ten healthy males (age 23.9 ± 2.7 years; height 1.83 ± 0.06 m; body mass 85.5 ± 17.4 kg) participated in the study. All participants provided informed consent and all procedures were approved by the institutional review board. Participants performed six maximum vertical jumps beginning from an initial squat position. Three were performed from the preferred starting position. The participants were then asked to perform three jumps from a self-selected deeper squat. During all jumps, the participants kept their hands on their hips, to eliminate arm motion. The participants warmed-up before testing, and rested for at least 1 min between jumps.

Kinematic data were obtained using a Pro-Reflex Motion Analysis System (Qualisys, Inc.), sampling at 240 Hz. Markers were placed on the following body landmarks: acromion process, great trochanter, lateral femoral condyle, lateral maleolus, and the base of the fifth metatarsal. Joint angles were defined so that all joint angles were zero in upright stance. Ground reaction force data were sampled synchronously with the motion analysis data using a force platform (N50601, Bertec Corporation, Worthington, Ohio), sampling at 1200 Hz.

Jump height was assumed to be the maximum vertical displacement of the centre of mass once contact was lost with the ground. It was computed from the centre of mass vertical take-off velocity, which was determined from the impulse obtained by integrating the vertical ground reaction force – time curve, less body weight, with respect to time. Jump time was measured as the time from movement initiation to take-off.

Resultant joint moments in the sagittal plane were computed for the ankle, knee, and hip joints (Winter, 1990). To determine these moments, the segmental inertial parameters were determined for each participant by modelling their segments as series of geometric solids (Yeadon, 1990). The densities of these segments were derived from the cadaver data of Clauser, McConville and Young (1969). Moments were defined so that those causing joint extension were positive. The moments for each participant were normalized with respect to the product of the participant's body weight and height.

From the time histories of the joint angles, angular velocities, and resultant moments, the initial posture joint angles and maximum joint velocities and moments were extracted for further analysis, as well as the timing of these events expressed as time before take-off. Two-factor repeated-measures multivariate analysis of variance was used to compare jump height, jump time, initial posture joint angles, and maximum joint angular velocities and moments under both conditions. For all statistical comparisons, statistical significance was set at $P < 0.05$. Homogeneity of variance was confirmed before performing the analysis of variance using a Bartlett test.

Model analysis

A direct dynamics simulation model was used to simulate jumps from different starting postures. The jumps were simulated using an optimal control direct dynamics muscle moment driven model. The model used was similar to others used to examine jumping (e.g. Van Soest *et al.*, 1993). The model had four rigid links (foot, shank, thigh, and a combined head, arms, and trunk), connected by frictionless hinge joints. The foot was connected to the ground by a hinge joint at the metatarsal – phalangeal joint, with a rotational spring-damper at this joint to represent the floor – heel interaction (Selbie & Caldwell, 1996). The equations of motion were formulated as mixed differential-algebraic equations (Haug, 1989). The equations of motion for the model relate the moments at the joints to the kinematics of the segments. These equations can be written as

$$\ddot{\boldsymbol{\theta}} = \boldsymbol{M}(\boldsymbol{\theta})^{-1}(\boldsymbol{M}_{\mathbf{J}} - \boldsymbol{v}(\boldsymbol{\theta}, \dot{\boldsymbol{\theta}}) - \boldsymbol{G}(\boldsymbol{\theta})) \qquad (1)$$

where $\ddot{\boldsymbol{\theta}}$ is the vector of joint angular accelerations, $\boldsymbol{M}(\boldsymbol{\theta})$ is the inertia matrix, $\boldsymbol{M}_{\mathbf{J}}$ is the vector of joint moments, $\boldsymbol{v}(\boldsymbol{\theta}, \dot{\boldsymbol{\theta}})$ is the vector of centrifugal and Coriolis terms, and $\boldsymbol{G}(\boldsymbol{\theta})$ is the vector of gravity terms.

The inertial parameters for the model's links were the same as those for a typical participant. The equations of motion for these links were integrated forwards in time using the improved Euler method (Ross, 1989), with a 0.0001 s time step. Using a fifth-order Runge-Kutta to integrate the equations, or using a smaller time step, did improve simulation accuracy, and slowed the simulations.

The model was actuated by six muscle models representing the gastrocnemius, soleus, vastus group, rectus femoris, hamstrings group, and gluteal group. Each muscle was represented by a Hill-type model consisting of a series elastic element and a contractile element (see Appendix for more details). The contractile element had non-linear force – length

and force–velocity properties, with output scaled via an activation dynamics model. Muscle force scales as a linear function of activation level, which is determined, in a non-linear fashion, by the neural excitation sent to the model's muscles. Both active state and neural excitation are normalized, so that zero reflects no activity and one is maximal. During the simulations, the length and moment arm of each muscle were determined using the equations presented by Visser, Hoogkamer, Bobbert and Huijing (1990). These equations, which are based on cadaver data, permit determination of muscle length and moment arm given the angle at each of the joints a muscle crosses.

Initial estimates of muscle model parameters for the lower limb were based on Van Soest *et al.* (1993) and Friederich and Brand (1990); they were then adjusted to reflect the physique of a typical participant in this study. Table I provides a summary of the model parameters used in this study.

A genetic search algorithm (Goldberg, 1989) was used to select sequences of neural excitations sent to each modelled muscle. Such algorithms have good convergence to a global minimum (Rudolph, 1994). To ensure convergence to a global minimum, multiple random seedings of initial estimates of neural excitations were performed. The sequence of neural excitations was selected so that the model's total potential and vertical kinetic energy of the centre of mass were maximized at the instant the foot lost contact with the ground. The optimal control problem was converted into a static optimization problem (Goh & Teo, 1988), which was achieved by representing the time histories of neural excitation for each of the six muscles as a series of control nodes separated by 0.05 s. Neural excitation between these nodes was determined by linear interpolation. Neural excitation was constrained to be between 0 and 1.

The first value for each modelled muscle's neural excitation was selected so that the model would be in static equilibrium in the initial squat position. This was done by computing the resultant moments at the ankle, knee, and hip joints required for this squat position. The muscle forces required to produce these moments were computed in the following fashion. First, the contributions of the bi-articular muscles to each joint's resultant moment were allocated based on the fraction each of these muscles could contribute to a maximum isometric moment at the joints they crossed. The contributions of the mono-articular muscles were then computed so that the initial squat resultant joint moments were produced.

Jumps were simulated from a position that matched the preferred position of a typical participant in the present study. This position is referred to as the ''standard position''. The initial squat position that maximized jump performance was also determined. For this problem, the genetic search algorithm found the optimal initial segment angles as well as the neural excitations at the control nodes. Jump height and the time history of the model kinematics were analysed and compared with the participants for validation of the model.

Results

As in the Methods section, the results are divided into sub-sections detailing the experimental and modelling approaches.

Experimental analysis

There was a significant difference between initial positions of the centre of mass in the two conditions, deep and preferred squat depths. This was achieved by a marked increase in flexion at the knee and hip (Table II). The participants were consistent in their depth of squat: there were no differences in squat depth between the trials for a given condition. Ground contact time increased with squat depth, but there was no difference between jump heights from the preferred or deep postures (Table II).

There were no differences in the maximum joint moments between jump heights at the preferred or

Table I. Summary of the muscle model parameters.

	F_{max} (N)	$L_{F,opt}$ (m)	w (−)	L_{TR} (m)	C (ε)	V_{max} ($L_{F,opt}$/s)	k (−)
Soleus	13 500	0.076	0.56	0.226	0.04	5.2	2.44
Gastrocnemius	4500	0.050	0.56	0.350	0.04	5.2	2.44
Vasti group	15 000	0.128	0.56	0.14	0.04	5.2	2.44
Rectus femoris	3000	0.104	0.56	0.371	0.04	5.2	2.44
Hamstrings group	6750	0.245	0.56	0.154	0.04	5.2	2.44
Gluteal group	10 500	0.171	0.56	0.128	0.04	5.2	2.44

Note: F_{max} = maximum isometric force (values are for both legs), $L_{F,opt}$ = optimal fibre length, w = spread of the force–length curve, L_{TR} = resting length of tendon, C = tendon strain under maximum isometric force, V_{max} = maximum unloaded shortening velocity, and k = force–velocity curvature constant.

deep postures. However, the timing of the maximum joint moments at the knee and ankle occurred earlier in the jumps from the deep squat (Table III).

Model analysis

The kinematics of the simulated standard position squat jumps were similar to those produced by the participants, with joint extensions showing a proximal-to-distal sequence (Figure 1). The simulated jump from the standard position achieved a height of 0.19 m, which was within the range of jump heights achieved by the participants (Table II), with the jump height for the model from its optimal initial position being 0.26 m. Jump time for the model was 44% longer for the optimal initial position compared with the standard position. The optimal initial position was a much deeper squat than that obtained by any of the participants (90° of hip flexion, 105° of knee flexion, and 40° of dorsiflexion). This initial position reflected the minimum feasible by the model, reflecting the maximum range of motion of a human participant.

Neural excitation for the mono-articular muscles was similar for jumps for both squat depths. However, different neural excitation patterns were required for two of the three bi-articular muscles to produce optimal jumps from the two different starting positions. The hamstrings and the rectus femoris are more deactivated before take-off in jumps from a standard posture than they are in jumps from a deep posture (Figure 2).

Discussion

The participants in this study jumped the same height from their preferred depth of squat and from a deeper position. The model jumped a similar height to the participants, and with a similar coordination pattern, even though the model has to be a simplification of the human musculoskeletal system. The model was able to jump higher from a deeper squat position than from a squat depth, mirroring the preferred depth of the participants. Examination of model active states indicated similar coordination of the all of the muscles for both squat depths, except for the bi-articular hamstrings. This required change in muscle coordination to optimize jump height may explain why the participants did not jump higher from a deeper squat.

There are some key differences between the model and the participants. One major difference that could account for the different performances from deep squats is that the model is optimally controlled from

Table II. Centre of mass height, joint angles in the initial squat positions, and the corresponding jump heights and times for the two types of jump (mean ± *s*).

	Deep squat	Preferred
Centre of mass height (m)*	0.56 ± 0.07	0.68 ± 0.07
Hip angle (°)*	101.5 ± 17.2	73.4 ± 15.5
Knee angle (°)*	93.8 ± 16.0	74.7 ± 10.3
Ankle angle (°)	27.49 ± 7.16	26.46 ± 8.02
Jump height (m)	0.27 ± 0.06	0.27 ± 0.06
Jump time (s)*	0.47 ± 0.07	0.30 ± 0.07

*Significantly different ($P < 0.05$).

Table III. Normalized maximum joint moments and their times for each of the conditions (mean ± *s*).

	Deep squat	Preferred
Hip moment	3.19 ± 1.45	3.28 ± 1.47
Time of maximum hip moment (s)*	0.31 ± 0.05	0.25 ± 0.07
Knee moment	3.54 ± 1.51	3.50 ± 1.6
Time of maximum knee moment (s)*	0.31 ± 0.05	0.26 ± 0.04
Ankle moment	3.29 ± 1.54	3.32 ± 1.39
Time of maximum ankle moment (s)*	0.30 ± 0.05	0.26 ± 0.05

Note: Times are expressed as time before take-off. Joint moments are normalized by (100/body weight × height).
*Significantly different ($P < 0.05$).

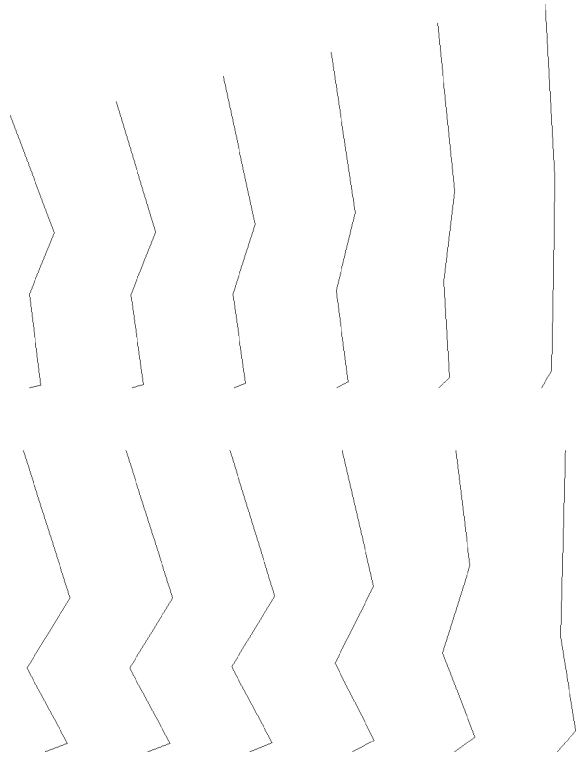

Figure 1. Stick figure comparing a representative participant (top) with the model (bottom) during the preferred squat depth jumps. The data are presented at 0.05-s intervals.

any starting posture, which is not necessarily true for the participants. Jumping from a deep squat is not often practised, so the participants presumably were not as well coordinated in the deep squats as they were from their preferred depth. An interesting observation is that a two-peak vertical ground reaction force pattern was seen in eight of the ten participants in jumps from the deep squat for each of the three trials. This was not seen in any of the jumps from the preferred starting posture. Figure 3 shows the vertical ground reaction force for jumps from both positions for a typical participant. The model is optimally coordinated and used a different coordination pattern for the bi-articular muscles in the two jumps. This could explain the different ground reaction force profiles, although this link cannot be established directly.

There are several reasons why the participants do not typically execute deep squat jumps. Several participants commented that jumps from the deep squats required more effort than squats from the preferred position. There is also likely an increased initial strain on the joints during jumps from deep squats (Shelburne & Pandy, 2002). In addition, in many sports the increased time for the deeper squat jump may be a disadvantage; although for the model this increase in time was not as large as it was for the experimental participants.

All models have to be parsimonious representations of the complex systems they seek to emulate.

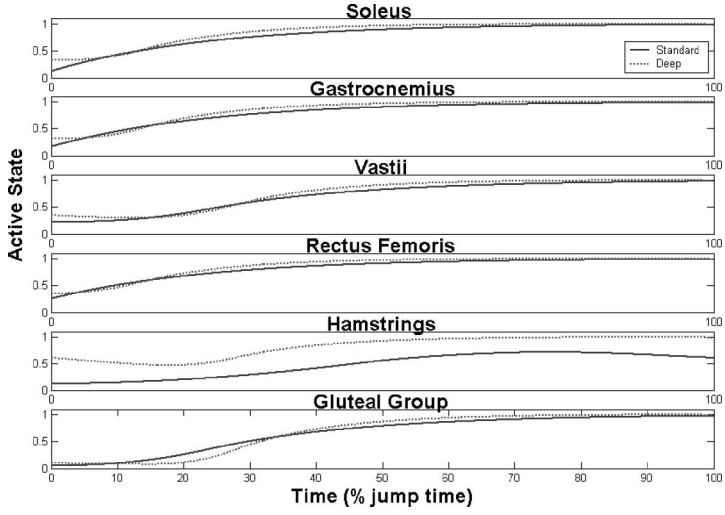

Figure 2. Active states for the muscles during both simulated jumps.

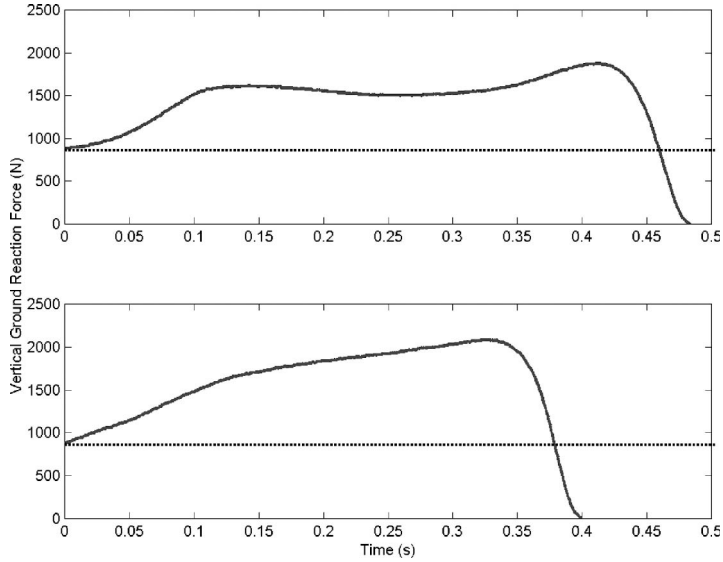

Figure 3. Vertical ground reaction force for a representative participant for jumps from the deep position (top) and preferred position (bottom). Body weight is shown by the dotted line.

The model used in the present study is similar in complexity to many models of jumping (e.g. Bobbert *et al.*, 1996), and is more complex than others (e.g. Alexander, 1990; Selbie & Caldwell, 1996). Many models of jumping have specified muscle neural excitation sequences by giving an initial neural excitation level, and then specifying a time when the muscle is either turned on to its maximum or turned off. The present model represented the time histories of neural excitation as a series of control nodes separated by 0.05 s, giving the opportunity for more subtle control of the muscles. In contrast, Van Soest *et al.* (1994) used the simpler activation scheme. Jumping simulations with their model suggested that humans use a similar activation pattern when jumping from a variety of starting positions. The current set of results suggests that their result may have been an artifact of their simple activation scheme.

There is evidence in the literature to suggest that motor unit activation varies with joint angle(s), particularly for bi-articular muscles (e.g. Babault, Pousson, Michault, & Van Hoecke, 2003; Christova, Kossev, & Radicheva, 1998; Maffiuletti & Lepers, 2003). There is also evidence that the same muscle can operate *in vivo* over different portions of the force–length curve for different participants (e.g. Herzog, Guimaraes, Anton, & Carter-Edman, 1991). The force–length properties of the model did not explicitly account for a force–length–activation relationship, nor was it used to examine the variations seen *in vivo* at the expressed section of the force–length curve. These were not explicitly included in the model, but the muscle force–length properties in the model were designed to produce typical moment–angle curves seen *in vivo* (Kulig, Andrews, & Hay, 1984), and so represent the output of a typical participant. If there was a reduction in the force produced by the muscles for the deeper depth squats, it would not invalidate the results obtained in the present study because to increase jump height the model only needs to pass through the preferred squat position with the muscles more activated, so the muscles only needed to have sufficient force-generating capacity to allow the participants to move through their preferred squat position. This should be considered the same mechanism as occurs in the performance enhancement in countermovement jumps, the longer duration of the tasks permitting the muscles to achieve greater activation (Bobbert *et al.*, 1996).

It was assumed that the tendons in the model had linear stress–strain properties and that for all the modelled muscles the tendon was equally extended under maximum isometric conditions. The first assumption is common in many muscle models (e.g. Zajac, 1989), yet there is evidence to suggest the tendon stress–strain properties are non-linear (e.g. Bennett, Ker, Dimery, & Alexander, 1986) but that tendon properties are reasonably approximated by a linear function above low forces (e.g. Alexander, 1988). The second assumption is very common in models of the musculoskeletal system (e.g. Nagano & Gerritsen, 2001; Pandy & Zajac, 1991; Van Soest *et al.*, 1993). There is a paucity of data on which to derive the amount of tendon strain under maximum isometric force for the muscles modelled in this study; but this is a necessary model parameter for a musculoskeletal model. Authors using ultrasound have reported tendon strain under maximum isometric force for the medial head of the gastrocnemius ranging from 8 to 11% (Kubo, Kanehisa, Kawakami, & Fukunaga, 2001; Magnusson *et al.*, 2003). Unfortunately, similar information does not exist for the other muscles represented in the model used in this study. To address potential concerns about the tendon model, in the musculoskeletal model the tendon model was replaced with a quadratic function, and the gastrocnemius tendon was permitted a maximum extension of 8% of its resting length under maximum isometric force. Simulations with the revised tendon model gave the same pattern of results as the original model, with the more elastic tendon increasing jump height by 10%. Bobbert (2001) has previously demonstrated that increasing tendon extension under maximum isometric force above 4% increases jump height. Irrespective of this performance increase, the influence of increased squat depth on vertical jump performance remained the same.

The experimental results show no change in jump height with increasing depth of squat, but the model did demonstrate an increased jump height. Given the theory explaining why countermovement jump height is greater than squat jump height (Bobbert *et al.*, 1996), it was anticipated that the deep squat jumps would achieve a greater height than the preferred squat depth jumps. The results from this study suggest that participants trained to jump from a deep squat position may be able to jump higher than from a preferred position, once the appropriate coordination is adopted. A future study will attempt to examine the influence of training on the ability to exploit additional squat depth, which may lead to the recommendation that athletes train to improve flexibility so that the option is available to achieve greater squat depths. While jumping from a deep squat is not practical for some activities, such a strategy may be viable for others and lead to enhanced performance.

Acknowledgement

This research was supported in part by a grant from The Whitaker Foundation.

References

Alexander, R. M. (1988). *Elastic mechanisms in animal movement.* Cambridge: Cambridge University Press.

Alexander, R. M. (1990). Optimum take-off techniques for high and long jumps. *Philosophical Transactions of the Royal Society of London B*, *329*, 3–10.

Babault, N., Pousson, M., Michaut, A., & Van Hoecke, J. (2003). Effect of quadriceps femoris muscle length on neural activation during isometric and concentric contractions. *Journal of Applied Physiology*, *94*, 983–990.

Bennett, M. B., Ker, R. F., Dimery, N. J., & Alexander, R. M. (1986). Mechanical properties of various mammalian tendons. *Journal of Zoology*, *209*, 537–548.

Bobbert, M. F. (2001). Dependence of human squat jump performance on the series elastic compliance of the triceps surae: A simulation study. *Journal of Experimental Biology*, *204*, 533–542.

Bobbert, M. F., Brand, C., de Hann, A., Huijing, P. A., Van Ingen Schenau, G. J., Rijnsburger, W. H. *et al.* (1986). Series elasticity of tendinous structures of the the rat EDL. *Journal of Physiology*, *377*, 89p.

Bobbert, M. F., Gerritsen, K. G. M., Litjens, M. C. A., & Van Soest, A. J. (1996). Why is countermovement jump height greater than squat jump height? *Medicine and Science in Sports and Exercise*, *28*, 1402–1412.

Challis, J. H. (1998). An investigation of the influence of bi-lateral deficit on human jumping. *Human Movement Science*, *17*, 307–325.

Challis, J. H., & Kerwin, D. G. (1994). Determining individual muscle forces during maximal activity: Model development, parameter determination, and validation. *Human Movement Science*, *13*, 29–61.

Christova, P., Kossev, A., & Radicheva, N. (1998). Discharge rate of selected motor units in human biceps brachii at different muscle lengths. *Journal of Electromyography and Kinesiology*, *8*, 287–294.

Clauser, C. E., McConville, J. T., & Young, J. W. (1969). Weight, volume and center of mass of segments of the human body. *AMRL Technical Report* (pp. 69–70). Wright Patterson Air Force Base, OH.

Fitzhugh, R. (1977). A model of optimal voluntary muscular control. *Journal of Mathematical Biology*, *4*, 203–236.

Friederich, J. A., & Brand, R. A. (1990). Muscle fiber architecture in the human lower limb. *Journal of Biomechanics*, *23*, 91–95.

Gallucci, J. G., & Challis, J. H. (2002). Examining the role of the gastrocnemius during the leg curl exercise. *Journal of Applied Biomechanics*, *18*, 15–27.

Goh, C. J., & Teo, K. L. (1988). Control parameterization: A unified approach to optimal control problems with general constraints. *Automatica*, *24*, 3–18.

Goldberg, D. E. (1989). *Genetic algorithms in search, optimization, and machine learning* (pp. 1–22). Reading, MA: Addison-Wesley.

Haug, E. J. (1989). *Computer aided kinematics and dynamics of mechanical systems, Vol. 1: Basic methods* (pp. 199–280). Boston, MA: Allyn & Bacon.

Herzog, W., Guimaraes, A. C., Anton, M. G., & Carter-Edman, K. A. (1991). Differences in the moment–length relations of rectus femoris muscles of speed skaters/cyclists and runners. *Medicine and Science in Sports and Exercise*, *23*, 1289–1296.

Hill, A. V. (1938). The heat of shortening and dynamic constants of muscle. *Proceedings of the Royal Society of London B*, *126*, 136–195.

Kubo, K., Kanehisa, H., Kawakami, Y., & Fukunaga, T. (2001). Influence of static stretching on viscoelastic properties of human tendon structures *in vivo*. *Journal of Applied Physiology*, *90*, 520–527.

Kulig, K., Andrews, J. G., & Hay, J. G. (1984). Human strength curves. *Exercise and Sport Sciences Reviews*, *12*, 417–466.

Maffiuletti, N. A., & Lepers, R. (2003). Quadriceps femoris torque and EMG activity in seated versus supine position. *Medicine and Science in Sports and Exercise*, *35*, 1511–1516.

Magnusson, S. P., Hansen, P., Aagaard, P., Brond, J., Dyhre-Poulsen, P., Bojsen-Moller, J. *et al.* (2003). Differential strain patterns of the human gastrocnemius aponeurosis and free tendon, *in vivo*. *Acta Physiologica Scandinavica*, *177*, 185–195.

Morgan, D. L., Proske, U., & Warren, D. (1978). Measurement of muscle stiffness and the mechanism of elastic storage in hopping kangaroos. *Journal of Physiology*, *282*, 253–261.

Nagano, A., & Gerritsen, K. G. M. (2001). Effects of neuromuscular strength training on vertical jumping performance – a computer simulation study. *Journal of Applied Biomechanics*, *17*, 113–128.

Pandy, M. G., Anderson, F. C., & Hull, D. G. (1992). A parameter optimization approach for the optimal control of large-scale musculoskeletal systems. *Journal of Biomechanical Engineering*, *114*, 450–460.

Pandy, M. G., & Zajac, F. E. (1991). Optimal muscular coordination strategies for jumping. *Journal of Biomechanics*, *24*, 1–10.

Ross, S. L. (1989). *Introduction to ordinary differential equations* (pp. 449–454). New York: Wiley.

Rudolph, G. (1994). Convergence analysis of canonical genetic algorithms. *IEEE Transactions on Neural Networks*, *5*, 96–101.

Scott, S. H., & Winter, D. A. (1991). A comparison of three muscle pennation assumptions and their effect on isometric and isotonic force. *Journal of Biomechanics*, *24*, 163–167.

Selbie, W. S., & Caldwell, G. E. (1996). A simulation study of vertical jumping from different starting postures. *Journal of Biomechanics*, *29*, 1137–1146.

Shelburne, K. B., & Pandy, M. G. (2002). A dynamic model of the knee and lower limb for simulating rising movements. *Computer Methods in Biomechanics and Biomedical Engineering*, *5*, 149–159.

Van Soest, A. J., Bobbert, M. F., & Van Ingen Schenau, G. J. (1994). A control strategy for the execution of explosive movements from varying starting positions. *Journal of Neurophysiology*, *71*, 1390–1402.

Van Soest, A. J., Schwab, A. L., Bobbert, M. F., & Van Ingen Schenau, G. J. (1993). The influence of the biarticularity of the gastrocnemius muscle on vertical-jumping achievement. *Journal of Biomechanics*, *26*, 1–8.

Visser, J. J., Hoogkamer, J. E., Bobbert, M. F., & Huijing, P. A. (1990). Length and moment arm of the human leg muscles as a function of knee and hip joint angles. *European Journal of Applied Physiology*, *61*, 453–460.

Winter, D. A. (1990). *Biomechanics and motor control of human movement.* Chichester, UK: Wiley.

Woittiez, R. D., Huijing, P. A., Boom, H. B. K., & Rozendal, R. H. (1984). A three-dimensional muscle model: A quantified relation between form and function of skeletal muscle. *Journal of Morphology*, *182*, 95–113.

Yeadon, M. R. (1990). The simulation of aerial movement, II: A mathematical inertia model of the human body. *Journal of Biomechanics*, *23*, 67–74.

Zajac, F. E. (1989). Muscle and tendon: properties, models, scaling, and application to biomechanics and motor control. *Critical Reviews in Biomedical Engineering*, *17*, 359–411.

Appendix

The model of human skeletal muscle used in this study is phenomenological in nature, with the model's contractile component representing the action of the muscle fibres and the series elastic component representing the tendon (Challis & Kerwin, 1994; Gallucci & Challis, 2002). The model ignores the influence of muscle pennation, an assumption supported previously (e.g. Scott & Winter, 1991). The force produced by the muscle model (F_M) is dependent on four factors, which are represented in the following equation:

$$F_M = q \cdot F_{max} \cdot F_L(L_F) \cdot F_V(V_F) \qquad (A1)$$

where q is the current active state of the muscle model, F_{max} is the maximum isometric force possible by the muscle model, $F_L(L_F)$ is the fraction of the normalized force–length curve that the model can produce at its current fibre length (L_T), and $F_V(V_F)$ is the fraction of the normalized force–velocity curve that the model can produce at its current fibre velocity (V_F).

The normalized force–length properties of the contractile component of the muscle model were represented by

$$F_L(L_F) = 1 - \left(\frac{(L_F - L_{F,opt})}{w \cdot L_{F,opt}}\right)^2 \qquad (A2)$$

where $L_{F,opt}$ = the optimum length of muscle fibre, which is the length at which the fibres can produce their maximum force, and w is a parameter indicating the spread of the force–length curve.

The force–velocity properties vary depending on whether the muscle is behaving concentrically or eccentrically. These parts were separately modelled based equations presented by Hill (1938) and Fitzhugh (1977) respectively:

$$F_V(V_F) = \frac{(V_{F,max} - V_F)}{(V_{F,max} + k \cdot V_F)} \qquad V_F \geq 0 \qquad (A3)$$

$$F_V(V_F) = 1.5 - 0.5\frac{(V_{F,max} + V_F)}{(V_{F,max} - 2 \cdot k \cdot V_F)} \qquad V_F < 0 \qquad (A4)$$

where $V_{F,max}$ is maximum muscle fibre velocity and k is the model shape parameter.

In series with the contractile component is an elastic component, which assumes that the tendon has a linear stress–strain curve. The force–extension curve of this element is represented by

$$L_T = L_{TR} + \frac{c}{F_{max}} \cdot L_{TR} \cdot F_M \qquad (A5)$$

where L_T is the current length of the tendon, L_{TR} is the resting length of the tendon, and c is the extension of a tendon under maximum isometric force as a fraction of its tendon resting length.

The assumption of linearity of the stress–strain curve is supported by data in the literature, as is a fixed value of c (e.g. Bobbert *et al.*, 1986; Morgan, Proske, & Warren, 1978; Woittiez, Huijing, Boom, & Rozendal, 1984). The typical value of c often reported in the literature is 0.04, implying the tendon will stretch by 4% of its resting length under a maximum isometric force.

The active state is a function of the neural excitation of the muscle (u). The muscle active state represents the recruitment as well as the firing rate, or rate coding, of the α-motorneurons. The active state is normalized so that zero represents no activation and one represents maximum activation. The relationship between the neural excitation and the active state is represented by a first-order differential equation presented by Pandy, Anderson and Hull (1992):

$$\dot{q} = \frac{1}{t_{rise}} \cdot (u - q) \cdot u + \frac{1}{t_{fall}} \cdot (u - (q - q_{min}) - (u - q) \cdot u) \qquad (A6)$$

where $\dot{q}$ is the rate of change of the active state of a muscle, q is the active state of a muscle after a time interval ($0 \leq q \geq 1$), t_{rise} and t_{fal} are constants associated with the increase (20 ms) and decrease in active state (5 ms) respectively, u is the current level of neural excitation ($0 \leq u \geq 1$), and q_{min} is the minimum level of active state (0.005). The variable q_{min} is required to eliminate instabilities in the ordinary differential equation for values near zero.

The simulation process was based around the iterative solving of the following first-order ordinary differential equation:

$$\frac{dF_M}{dt} = K(V_{MT} - V_F) = K \cdot V_T \qquad (A7)$$

where the rate of change of the muscle force is equal to the product of the tendon stiffness (K) and the velocity of the tendon (V_T), and the velocity of the tendon is equal to the difference between muscle–tendon velocity (V_{MT}) and muscle fibre velocity (V_T). The tendon stiffness is just the gradient of the slope of the force–extension curve for the model of the series elastic component (equation A5).